Journal of Biomolecular NMR (2006) 36:259–266
DOI 10.1007/s10858-006-9090-1

Article

^{13}C-detected HN(CA)C and HMCMC experiments using a single methyl-reprotonated sample for unambiguous methyl resonance assignment

Kaifeng Hu†, Beat Vögeli† & G. Marius Clore*
Laboratory of Chemical Physics, National Institute of Diabetes and Digestive and Kidney Diseases, National Institutes of Health, Bethesda, MD 20892-0520, USA

Received 23 July 2006; Accepted 14 September 2006

Key words: ^{13}C-detected NMR spectroscopy, methyl resonance assignment, IIB^{Mannose}

Abstract

Methyl groups provide an important source of structural and dynamic information in NMR studies of proteins and their complexes. For this purpose sequence-specific assignments of methyl ^{1}H and ^{13}C resonances are required. In this paper we propose the use of ^{13}C-detected 3D HN(CA)C and HMCMC experiments for assignment of methyl ^{1}H and ^{13}C resonances using a single selectively methyl protonated, perdeuterated and ^{13}C/^{15}N-labeled sample. The high resolution afforded in the ^{13}C directly-detected dimension allows one to rapidly and unambiguously establish correlations between backbone H_N strips from the 3D HN(CA)C spectrum and methyl group H_mC_m strips from the HMCMC spectrum by aligning all possible side-chain carbon chemical shifts and their multiplet splitting patterns. The applicability of these experiments for the assignment of methyl ^{1}H and ^{13}C resonances is demonstrated using the 18.6 kDa B domain of the *Escherichia coli* mannose transporter (IIB^{Mannose}).

Introduction

Resonance assignments are central to NMR studies of protein structure and dynamics (Wuthrich, 1986; Clore and Gronenborn, 1991, 1998; Mittermaier and Kay, 2006). Methyl groups are important reporters of dynamics in relaxation studies (Kay, 2005) and NOEs involving methyl groups yield invaluable information for structure determination of proteins (Kay, 2005) and their complexes (Williams et al., 2005; Suh et al., 2006). Sequence-specific assignments of methyl ^{1}H and ^{13}C resonances are therefore an essential prerequisite for many NMR studies. Previously, 3D HCCH-COSY (Bax et al., 1990a; Kay et al., 1990) and HCCH-TOCSY (Bax et al., 1990b; Fesik et al., 1990; Olejniczak et al., 1992) experiments via isotropic mixing of ^{13}C magnetization have been widely used for side-chain ^{1}H and ^{13}C resonance assignment in protonated proteins. Conventional ^{1}H detected COSY-based NMR experiments have also been developed for the assignment of methyl ^{1}H and ^{13}C chemical shifts of Ile, Leu and Val residues in a large perdeuterated protein, malate synthase G, in which the Ile, Leu and Val residues were $^{13}CH_3$-labeled at only a single methyl position, with the other methyl group $^{12}CD_3$-labeled (Tugarinov et al., 2003). This special methyl group labeling scheme is required to "linearize" the spin systems for efficient coherence transfer. In the

†These two authors contributed equally to this work.

*To whom correspondence should be addressed. E-mail: mariusc@intra.niddk.nih.gov

experiments described by Tugarinov et al. (2003), selective pulses are repeatedly applied and their phases have to be adjusted. The "out-and-back" approach also requires many INEPT elements, leading to additional signal loss. A constant-time MQ-(H)CC$_m$H$_m$-TOCSY experiment has been proposed for sequence-specific assignments of methyl groups using a large uniformly ^{13}C-labeled protein (Yang et al., 2004). However, for some Leu residues with strong scalar coupling between $^{13}C^{\delta 1}/^{13}C^{\delta 2}$ and $^{13}C^{\gamma}$, this experiment is less sensitive due to incomplete refocusing of the ^{13}C magnetization during the constant time period.

The first 2D ^{13}C-detected spectrum for protein sequence-specific assignment was reported by Markley and coworkers (Oh et al., 1988). Recently, ^{13}C-detected NMR spectroscopy has been proposed as an attractive alternative for studying large macromolecules (Bermel et al., 2003, 2006; Eletsky et al., 2003; Hu et al., 2003, 2005; Bertini et al., 2004; Kovacs et al., 2005). In this paper, we propose the use of ^{13}C-detected 3D HN(CA)C and HMCMC TOCSY-type experiments for assignment of methyl ^{1}H and ^{13}C resonances using a single methyl protonated, highly deuterated, ^{13}C/^{15}N-labeled protein sample. These ^{13}C-detected spectra offer high resolution and the observation of all side-chain carbon chemical shifts in the direct ^{13}C dimension. Correlation between methyl groups and their backbone H$_N$ groups is established via alignment of all observed side-chain carbon chemical shifts and their multiplet splitting pattern in the ^1H_N–^{13}C strips from the 3D HN(CA)C spectrum and in the ^1H_m–^{13}C strips from the 3D HMCMC spectrum (Figure 1), which affords unambiguous assignment of methyl resonances. These ^{1}H-start, ^{13}C-detect experiments make use of magnetization originating from ^{1}H spins (H$_N$ of amide groups and H$_m$ of methyl groups) and can therefore be expected to have higher sensitivity compared to 2D ^{13}C-start, ^{13}C-observe NMR experiments (Eletsky et al., 2003). Using methyl reprotonated, perdeuterated protein samples offers three times the initial magnetization while relaxation of deuterated carbons is minimized. The experiments are demonstrated using the 18.6 kDa ^{15}N/^{13}C/^{2}H/[Leu,Val]-methyl-protonated B domain (IIB^{Man}) of the *Escherichia coli* mannose transporter. The ^{13}C-detected "out-and-stay" 3D HN(CA)C and HMCMC experiments proposed here offer a general route for the unambiguous assignment of methyl ^{13}C and ^{1}H chemical shifts of high molecular weight ^{15}N/^{13}C/^{2}H-labeled, methyl selectively protonated proteins.

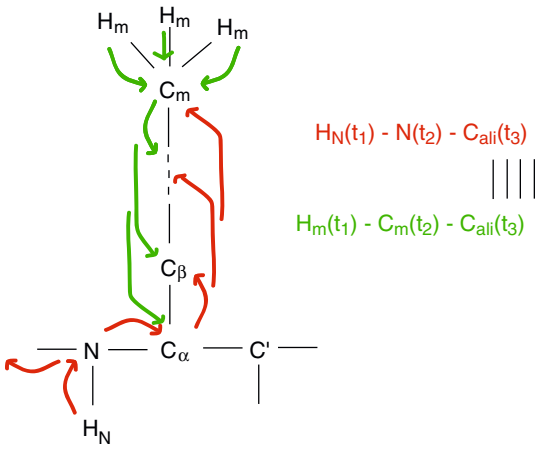

Figure 1. Schematic representation of the coherence transfer pathways observed in the 3D ^{13}C-directly detected HMCMC-TOCSY (green) and HN(CA)C-TOCSY (red) experiments. Correlation between methyl groups and their backbone H$_N$ groups is established via alignment of all side-chain carbon chemical shifts and their multiplet splitting patterns.

Material and methods

NMR sample preparation

The B domain (IIB^{Man}) of the *E. coli* mannose transporter, residues 156–322, was cloned into a modified pET-32a vector (Legler et al., 2004) to form a thioredoxin fusion protein with a His$_6$-tag. After transformation, *E. coli* strain BL21(DE3) (Novagen) was cultured in Luria Bertini medium, then adapted and grown in minimal medium in ^2H_2O using 1 g/l of $^{15}NH_4Cl$ and 2 g/l of $^2H_7/^{13}C_6$-glucose (Cambridge Isotope Laboratories) as the sole nitrogen and carbon sources, respectively. One hour prior to induction (at $A_{600} \sim 0.6$–0.7) with 1 mM isopropyl-D-thiogalactopyranoside, 50 mg 3-^{2}H, $^{13}C_5$-α-ketoisovaleric acid (Cambridge Isotope Laboratories) was added as precursor for Leu and Val reprotonation at their methyl groups. The cells were grown overnight and harvested. The cell pellet was resuspended in 150 ml (per liter of culture) of 20 mM Tris, pH 8.0, 150 mM NaCl. The suspension was lysed using a microfluidizer and centrifuged at 10,000 × *g* for

20 min. The supernatant was loaded onto a nickel-Sepharose column (Amersham Biosciences), and the fusion protein was eluted with a 150 ml gradient of imidazole (25–500 mM). The fusion protein was then digested with thrombin (100 units) and dialyzed in 20 mM Tris, pH 8.0, 200 mM NaCl. After addition of 1 mM phenylmethylsulfonyl fluoride, the cleaved His_6-thioredoxin was removed by loading the digested proteins over a nickel–Sepharose column. The IIB^{Man} fractions were collected and further purified by Sephadex-75 gel filtration column (Amersham Biosciences) equilibrated with 20 mM Tris, pH 7.4, 1 mM EDTA. The final $^{15}N/^{13}C/^{2}H$/[Leu,Val]-methyl-protonated IIB^{Man} NMR sample was concentrated to 0.7 mM in 20 mM phosphate buffer, pH 6.5 containing 0.01% (w/v) sodium azide and 8% $^{2}H_2O$.

NMR experiments

NMR experiments were performed at 308 K on a Bruker AVANCE 800 MHz spectrometer equipped with a cryogenic z-gradient DUL $^{13}C\{^{1}H\}$ probe. NMR data were processed with the program NMRPipe (Delaglio et al., 1995).

Results and discussion

NMR pulse sequences

Figure 2 shows the pulse schemes for the 3D HMCMC and HN(CA)C TOCSY-type experiments.

The HMCMC-TOCSY experiment (Figure 2A) is a $^{1}H^{methyl}$-resolved [$^{13}C^{methyl}$, $^{13}C^{ali}$]-TOCSY experiment, which is a modified version of the original 3D HCC-TOCSY (Hu et al., 2005) aimed at optimal performance for deuterated, methyl-reprotonated samples. While preparing this paper, a similar pulse sequence was published (Jordan et al., 2006). The initial $^{1}H^{methyl}$ polarization is excited and evolved to anti-phase coherence under scalar coupling with $^{13}C^{methyl}$ during a semi-constant time INEPT step while chemical-shift labelling $^{1}H^{methyl}$ (t_1). Subsequent 90° pulses on $^{1}H^{methyl}$ and $^{13}C^{methyl}$ create transverse anti-phase $^{13}C^{methyl}$ magnetization, followed by a second semi-constant time element with chemical-shift labelling of $^{13}C^{methyl}$ (t_2). The second semi-constant time aims to refocus $^{13}C^{methyl}$ magnetization into the in-phase form with respect to all three attached methyl protons. The optimal effective evolution time under three J_{HC}-couplings is approximately $1/(5J_{HC})$ (Cavanagh et al., 1996). Subsequent transfer of the in-phase $^{13}C^{methyl}$ magnetization to all aliphatic ^{13}C spins is achieved via an isotropic FLOPSY-16 sequence (Kadkhodaie et al., 1991; Eletsky et al., 2003). The 90° cleaning pulse on ^{1}H after the TOCSY mixing period converts residual anti-phase ^{13}C magnetization into unobservable multiple quantum coherences. ^{1}H and ^{2}H decoupling is applied during acquisition. ^{15}N decoupling is not applied because a substantial amount of signal is lost due to heteronuclear interference between ^{2}H, ^{15}N and ^{13}C frequencies (Vogeli et al., 2005).

In the 3D HN(CA)C TOCSY experiment (Figure 2B), the $^{1}H_N(i)$ polarization is excited and followed by a semi-constant time INEPT step while chemical-shift labeling $^{1}H_N$ (t_1). Subsequent 90° pulses on $^{1}H^N$ and ^{15}N transfer magnetization to $^{15}N(i)$. The ^{15}N (t_2) chemical shift is labeled in a constant time element while in-phase magnetization on $^{15}N(i)$ is generated via its scalar coupling to $^{1}H_N$ and by refocusing of $^{13}C^{ali}$ and $^{13}C'$ spins. The total duration of this element is determined by the desired resolution. In-phase to in-phase magnetization transfer from $^{15}N(i)$ to $^{13}C^{\alpha}(i)$ and $^{13}C^{\alpha}(i-1)$ is achieved via heteronuclear cross polarization (HCP) for a duration of 56 ms (Richardson et al., 1993). Transfer efficiency by HCP is comparable to in-phase to in-phase transfer using two consecutive INEPT steps. Relaxation depends on spin-system specific parameters, but is expected to be about equal (Ernst et al., 1991). However, during the application of the DIPSI-2 pulse train (Shaka et al., 1988), HCP already initiates in-phase to in-phase transfer from $^{13}C^{\alpha}$ to neighbouring ^{13}C spins. Therefore, the subsequent FLOPSY-16 mixing time can be substantially shortened. Here, we decrease the mixing time from 15.9 ms to 10.6 ms. ^{1}H and ^{2}H decoupling is applied during acquisition.

Resonance assignment using 3D HN(CA)C and HMCMC experiments

To illustrate the application of these experiments for methyl ^{1}H and ^{13}C chemical shift assignments, Figure 3 shows data from the ^{13}C-detected 3D HN(CA)C and HMCMC spectra recorded on the

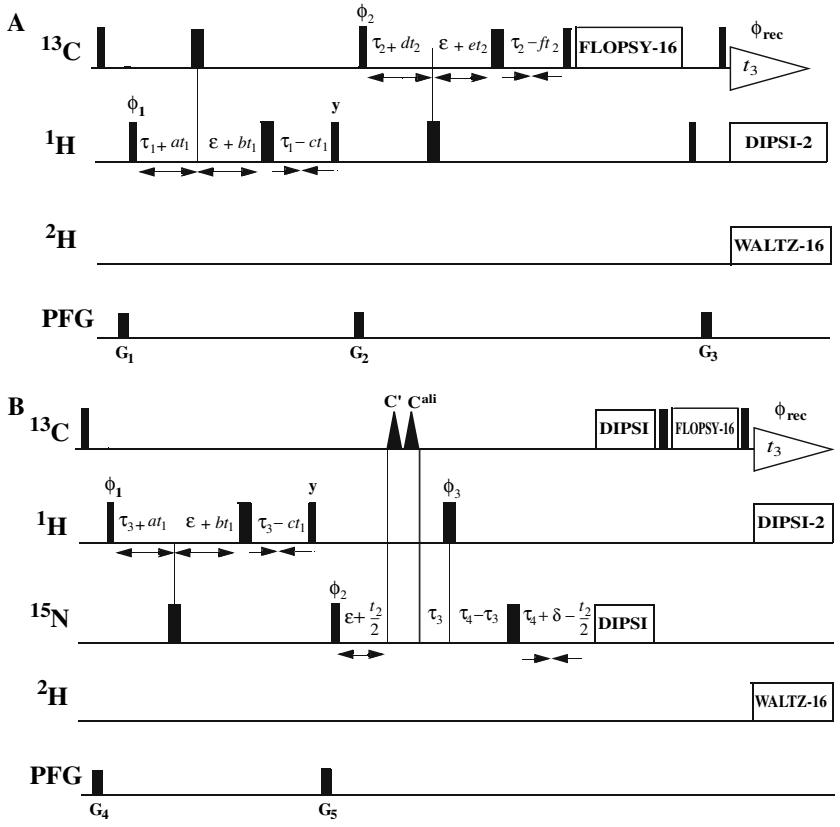

Figure 2. (A) 3D HMCMC-TOCSY and (B) 3D HN(CA)C-TOCSY pulse sequences for methyl group side-chain assignment. The carrier frequencies for ^{13}C, ^{1}H and ^{2}H pulses are set to 23 ppm (last ^{13}C-pulse and FLOPSY at 37 ppm), 0.8 ppm and 3.0 ppm, respectively, in (A) and to 58 ppm (last ^{13}C-pulse and FLOPSY at 40 ppm), 4.7 ppm and 3.0 ppm, respectively, in (B). The carrier frequency for the ^{15}N pulses is set to 118 ppm. Narrow and wide bars indicate non-selective 90° and 180° pulses, respectively, and triangles represent selective 180° rectangular pulses. The last ^{1}H pulse in (A) converts unwanted magnetization into unobservable multiple-quantum coherences. ^{1}H- and ^{2}H-decoupling is achieved with DIPSI-2 and WALTZ-16 pulse trains using field strengths γB_1 of 1.25 kHz and 0.625 kHz, respectively. DIPSI (γB_1 = 2.083 kHz) and FLOPSY (γB_1 = 8.333 kHz) mixing are applied for 56 ms and 15.9 ms (A)/10.6 ms (B), respectively. The delays are as follows: $\tau_1 = 1/(4J_{HC}) = 1.85$ ms, $\tau_2 = 1/(10J_{HC}) = 0.72$ ms, $\tau_3 = 1/(4J_{HN}) = 2.65$ ms, $\tau_4 > t_{max}(^{15}N)/2$, $\varepsilon = 2$ μs and $\delta = p_H + 2p_C + 2$ μs, where p_H and p_C are the pulse lengths of the 180° ^{1}H and selective ^{13}C pulses, respectively. Pulsed field gradients indicated on the line marked PFG are applied along the *z*-axis with durations and strengths as follows: G_1, 300 μs and 30 G/cm; G_2, 300 μs and 30 G/cm; G_3, 300 μs and 30 G/cm; G_4, 600 μs and 30 G/cm; and G_5, 600 μs and 30 G/cm. Unless indicated otherwise, all radio-frequency pulses are applied with phase *x*. The phase cycles are as follows: in (A) $\phi_1 = \{x,-x\}$, $\phi_2 = \{x, x,-x,-x\}$, and $\phi_{rec} = \{x,-x,-x, x\}$; in (B) $\phi_1 = \{x,-x\}$, $\phi_2 = \{y, y,-y,-y\}$, $\phi_3 = \{x, x, x, x,-x,-x,-x,-x, y, y, y, y,-y,-y,-y,-y\}$, and $\phi_{1rec} = \{x,-x,-x, x, x,-x,-x, x,-x, x, x,-x,-x, x, x,-x\}$. Incrementations follow the rules: $b = a - c$ and $\varepsilon = d - f$. The ^{1}H and ^{13}C chemical shifts evolve effectively during $2at_1$ and $2dt_2$. Quadrature detection in the $^{1}H(t_1)$, $^{13}C(t_2)$ (in A) and $^{15}N(t_2)$ (in B) dimensions is achieved using States-TPPI (Marion et al., 1989) applied to the phases ϕ_1 and ϕ_2, respectively, together with ϕ_{rec}.

18.6 kDa $^{15}N/^{13}C/^{2}H$/[Leu, Val]-methyl-protonated IIB^{Man}.

Figure 3A show $^{1}H_m$–^{13}C strips for $^{13}C^{\gamma 1}$ and $^{13}C^{\gamma 2}$ (middle and right panels) from the 3D ^{13}C-detected HMCMC spectrum and a $^{1}H_N$–^{13}C strip (left panel) from the ^{13}C-detected 3D HN(CA)C spectrum for Val-133. The alignment of the direct dimension $^{13}C^{\beta}$ and two $^{13}C^{methyl}$ chemical shifts in these strips relates the methyl groups to their backbone H_N group. Figure 3B and D show the detailed peak pattern matching in the expanded regions corresponding to the $^{13}C^{\beta}$ and $^{13}C^{m}$ chemical shifts of Val-133. In Figure 3C and E, 1D slices are extracted to align their multiplet splitting patterns and the corresponding side-chain carbon assignments are indicated. The expanded regions and 1D slices from the HN(CA)C spectrum in Figure 3F and G show the correlation to intra- and inter-residue $^{13}C^{\alpha}$ chemical shifts and to the $^{13}C^{\beta}$

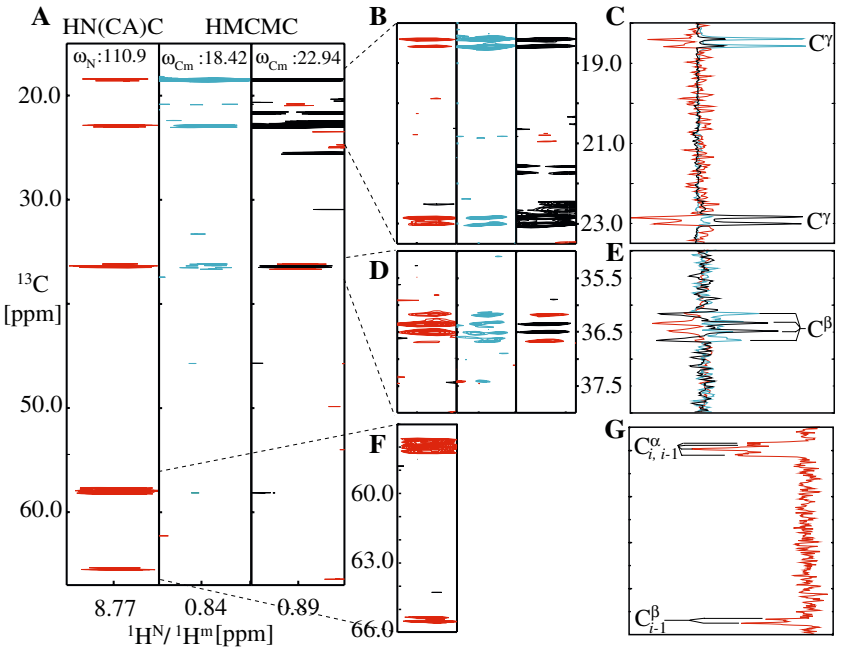

Figure 3. (A) H_N strip taken from the 3D ^{13}C-detected HN(CA)C-TOCSY spectrum and H_mC_m strips taken from the 3D HMCMC spectrum for Val-133 of $^{15}N/^{13}C,/^{2}H$/[Leu,Val]-methyl-protonated IIB^{Man}. The corresponding indirect $^{15}N/^{13}C$ chemical shifts are indicated at the top of each strip. Chemical shifts of the $^{13}C^{\beta}$ and two $^{13}C^{\gamma}$ resonances are aligned. (B) and (D) show the multiplet pattern for these carbons. (F) Expanded region shows the multiplet pattern of the intraresidue $^{13}C^{\alpha}$ correlation and the interresidue $^{13}C^{\alpha}$ and $^{13}C^{\beta}$ correlations to the preceding residue (Ser-132). (C), (E) and (G) Slices taken along the direct ^{13}C dimension are expanded to show the resolved multiplets due to J_{CC} couplings. Alignment of the splitting pattern resolved at the high resolution obtained in the directly detected ^{13}C dimension helps to confirm the assignment of the methyl resonances. The assigned carbons are labeled. The experiments were recorded at 800 MHz. For the HMCMC experiment, $35(t_1) \times 33(t_2) \times 2048(t_3)$ complex points were accumulated, with $t_{1max}(^{1}H_m)$ = 54.68 ms, t_{2max}(indirect $^{13}C_m$) = 16.4 ms and t_{3max}(direct ^{13}C) = 168.7 ms with 64 scans per increment. For the HN(CA)C experiment, $28(t_1) \times 31(t_2) \times 2048(t_3)$ complex points were accumulated, with $t_{1max}(^{1}H_N)$ = 10.94 ms, $t_{2max}(^{15}N)$ = 15.29 ms and t_{3max}(direct ^{13}C) = 168.7 ms with 112 scans per increment. Both experiments were run with an interscan delay of 0.9 s resulting in total experiment times of 92 h and 120 h for the 3D HMCMC-TOCSY and HN(CA)C-TOCSY experiments, respectively.

chemical shift of the preceding residue (Ser-132). The disappearance of the $^{13}C^{\alpha}$ peak in the two H_mC_m strips from the 3D ^{13}C-detected HMCMC spectrum is probably due to the absence of ^{15}N decoupling and the scalar couplings between $^{13}C^{\alpha}$ and $^{13}C^{\beta}$, $^{13}C'$. The observed splitting pattern in the directly detected ^{13}C dimension helps identification of residue type and assignment of side-chain carbon resonances. For example, the $^{13}C^{\beta}$ and $^{13}C^{\gamma 1/\gamma 2}$ resonances of Val appear as a quadruplet and doublet, respectively (Figure 3); while the $^{13}C^{\beta}$, $^{13}C^{\gamma}$ and $^{13}C^{\delta 1/\delta 2}$ resonances of Leu appear as a triplet, quadruplet and doublet, respectively (Figure 4). Alignment of these splitting patterns resolved at the high resolution obtained in the directly detected ^{13}C dimension helps to confirm the assignment of the methyl resonances.

To further demonstrate the application of these experiments for unambiguous methyl resonance assignment, an expanded crowded region of a ^{1}H-detected constant time (CT) ^{13}C-HMQC spectrum recorded on the same sample is shown in Figure 4A. For comparison, the overlaid cross-section of the 3D ^{13}C-detected HMCMC spectrum for the corresponding region is shown in Figure 4B, and clearly exhibits much higher resolution. To illustrate the assignment strategy employed for these methyl resonances, strips corresponding to Leu-57 and Leu-23 are taken as examples (Figure 4C and E), as indicated by the open dashed arrows. These strips can be almost perfectly aligned with the other methyl $^{1}H_m$–^{13}C strip from the same residues at the two $^{13}C^{\delta 1}/^{13}C^{\delta 2}$ chemical shifts and also at their $^{13}C^{\gamma}$ chemical shift. The horizontal dashed lines in Figure 4C and

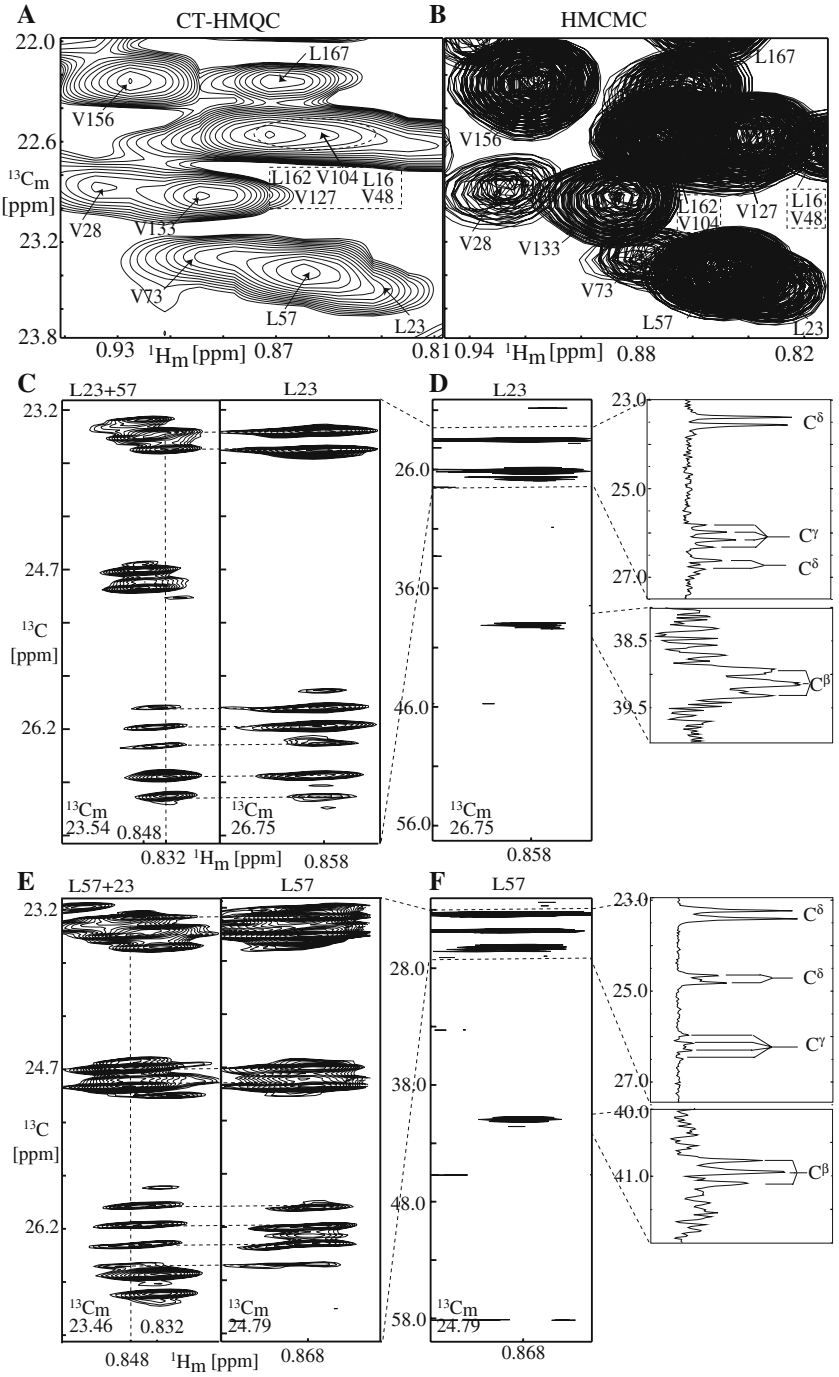

Figure 4. (A) An expanded region from the 2D ^{13}C CT-HMQC spectrum of $^{15}N/^{13}C/^{2}H$/[Leu, Val]-methyl-protonated IIB^{Man}. (B) Overlaid cross-sections of the H_mC_m planes of the 3D ^{13}C-detected HMCMC-TOCSY spectrum showing the corresponding region for comparison. (C) and (E) H_mC_m strips taken from the 3D HMCMC spectrum corresponding to Leu-57 and Leu-23. The horizontal dashed lines indicate the alignment of the multiplet pattern of these carbons. (D) and (F) Zoom-out of (C) and (E) showing the full range of ^{13}C chemical shifts in the ^{13}C directly-detected dimension, including two $^{13}C^{\delta1}/^{13}C^{\delta2}$ resonances and $^{13}C^{\gamma}$ and $^{13}C^{\beta}$ resonances. 1D slices (the right-hand panels in D and F) taken at the position of the methyl resonances of Leu-57 and Leu-23 show clear peak splitting patterns at these carbons.

E indicate the alignment of the multiplet pattern for these peaks. The zoom-out shown in Figure 4D and F reveals the full range ^{13}C chemical shifts in the ^{13}C directly-detected dimension, including two $^{13}C^{\delta 1}/^{13}C^{\delta 2}$ chemical shifts and $^{13}C^{\gamma}$, $^{13}C^{\beta}$ chemical shifts. These chemical shifts allow unambiguous identification of these methyl groups. Further, 1D slices (the right panels in Figure 4D and F) taken at the position of these methyl resonances show a clear peak splitting pattern at these carbons. The splitting pattern can be used to further confirm the assignments. This strategy clearly demonstrates how one can obtain unambiguous assignment for two methyl resonances located in a very crowded region of the 2D ^{13}C CT-HMQC spectrum, which have only slight chemical shift differences in both dimensions, 0.848 ppm versus 0.832 ppm in the H_m dimension, and 23.46 ppm versus 23.54 ppm in C_m dimension. Following the same approach, the crowded cluster of methyl resonances for Leu-162, Val-104, Leu-16, Val-127 and Val-48 can also be unambiguously assigned (Figure 4B).

Concluding remarks

In this paper we have presented a robust approach for the direct assignment of methyl group resonances by linking them to backbone amide groups using a single sample and two 3D ^{13}C-detected experiments, namely the HMCMC-TOCSY and HN(CA)C TOCSY experiments. Alignment of all side-chain carbon chemical shifts together with their multiplet patterns can lead to unambiguous identification of methyl resonances. For high molecular weight proteins and protein complexes for which high deuteration levels are required, the new methods described could find wide application. The HMCMC pulse sequence can be readily incorporated into relaxation experiments probing methyl group dynamics. In addition, the measurement of C–C residual dipolar couplings in the highly resolved ^{13}C-directly detected dimension may yield further insights into side-chain structure and dynamics (Vogeli et al., 2004).

Acknowledgements

This work was supported by the intramural program of NIDDK, NIH (to G.M.C.). B.V. acknowledges a Fellowship from the Swiss National Science Foundation. We thank Dr. Dusty Baber for technical assistance at the spectrometer.

References

Bax, A., Clore, G.M., Driscoll, P.C., Gronenborn, A.M., Ikura, M. and Kay, L.E. (1990a) *J. Magn. Reson.*, **87**, 620–628.
Bax, A., Clore, G.M. and Gronenborn, A.M. (1990b) *J. Magn. Reson.*, **88**, 425–431.
Bermel, W., Bertini, I., Felli, I.C., Kummerle, R. and Pierattelli, R. (2003) *J. Am. Chem. Soc.*, **125**, 16423–16429.
Bermel, W., Bertini, I., Felli, I.C., Piccioli, M. and Pierattelli, R. (2006) *Prog. Nucl. Magn. Reson. Spect.*, **48**, 25–45.
Bertini, I., Felli, I.C., Kummerle, R., Moskau, D. and Pierattelli, R. (2004) *J. Am. Chem. Soc.*, **126**, 464–465.
Cavanagh, J., Fairbrother, W.J., Palmer, A.G. and Skelton, N.J. (1996) *Protein NMR Spectroscopy: Principles and Practice*, Academic Press, New York.
Clore, G.M. and Gronenborn, A.M. (1991) *Science*, **252**, 1390–1399.
Clore, G.M. and Gronenborn, A.M. (1998) *Trends Biotech.*, **16**, 22–34.
Delaglio, F., Grzesiek, S., Vuister, G.W., Zhu, G., Pfeifer, J. and Bax, A. (1995) *J. Biomol. NMR*, **6**, 277–293.
Eletsky, A., Moreira, O., Kovacs, H. and Pervushin, K. (2003) *J. Biomol. NMR*, **26**, 167–179.
Ernst, M., Griesinger, C., Ernst, R.R. and Bermel, W. (1991) *Mol. Phys.*, **74**, 219–252.
Fesik, S.W., Eaton, H.L., Olejniczak, E.T., Zuiderweg, E.R.P., McIntosh, L.P. and Dahlquist, F.W. (1990) *J. Am. Chem. Soc.*, **112**, 886–888.
Hu, K.F., Eletsky, A. and Pervushin, K. (2003) *J. Biomol. NMR*, **26**, 69–77.
Hu, K.F., Vogeli, B. and Pervushin, K. (2005) *J. Magn. Reson.*, **174**, 200–208.
Jordan, J.B., Kovacs, H., Wang, Y., Mobli, M., Luo, R., Anklin, C., Hoch, J.C. and Kriwacki, R.W. (2006) *J. Am. Chem. Soc.*, **128**, 9119–9128.
Kadkhodaie, M., Rivas, O., Tan, M., Mohebbi, A. and Shaka, A.J. (1991) *J. Magn. Reson.*, **91**, 437–443.
Kay, L.E. (2005) *J. Magn. Reson.*, **173**, 193–207.
Kay, L.E., Ikura, M. and Bax, A. (1990) *J. Am. Chem. Soc.*, **112**, 888–889.
Kovacs, H., Moskau, D. and Spraul, M. (2005) *Progr. Nucl. Magn. Reson. Spect.*, **46**, 131–155.
Legler, P.M., Cai, M.L., Peterkofsky, A. and Clore, G.M. (2004) *J. Biol. Chem.*, **279**, 39115–39121.
Marion, D., Ikura, M., Tschudin, R. and Bax, A. (1989) *J. Magn. Reson.*, **85**, 393–399.
Mittermaier, A. and Kay, L.E. (2006) *Science*, **312**, 224–228.
Oh, B.H., Westler, W.M., Darba, P. and Markley, J.L. (1988) *Science*, **240**, 908–911.
Olejniczak, E.T., Xu, R.X. and Fesik, S.W. (1992) *J. Biomol. NMR*, **2**, 655–659.
Richardson, J.M., Clowes, R.T., Boucher, W., Domaille, P.J., Hardman, C.H., Keeler, J. and Laue, E.D. (1993) *J. Magn. Reson. Series B*, **101**, 223–227.
Rosen, M.K., Gardner, K.H., Willis, R.C., Parris, W.E., Pawson, T. and Kay, L.E. (1996) *J. Mol. Biol.*, **263**, 627–636.

Schwieters, C.D., Kuszewski, J.J. and Clore, G.M. (2006) *Prog. Nucl. Magn. Reson. Spect.*, **48**, 47–62.
Shaka, A.J., Lee, C.J. and Pines, A. (1988) *J. Magn. Reson.*, **77**, 274–293.
Suh, J.Y., Cai, M.L., Williams, D.C. and Clore, G.M. (2006) *J. Biol. Chem.*, **281**, 8939–8949.
Tugarinov, V. and Kay, L.E. (2003) *J. Am. Chem. Soc.*, **125**, 13868–13878.
Vogeli, B., Kovacs, H. and Pervushin, K. (2004) *J. Am. Chem. Soc.*, **126**, 2414–2420.
Vogeli, B., Kovacs, H. and Pervushin, K. (2005) *J. Biomol. NMR.*, **31**, 1–9.
Williams, D.C., Cao, M.L., Suh, J.Y., Peterkofsky, A. and Clore, G.M. (2005) *J. Biol. Chem.*, **280**, 20775–20784.
Wuthrich, K. (1986) *NMR of Proteins and Nucleic Acids*, Wiley, New York.
Yang, D.W., Zheng, Y., Liu, D.J. and Wyss, D.F. (2004) *J. Am. Chem. Soc.*, **126**, 3710–3711.